

Physical Layer Deception in OFDM Systems

Wenwen Chen*, Bin Han*, Yao Zhu[†], Anke Schmeink[†], and Hans D. Schotten*[‡]

*RPTU Kaiserslautern-Landau, *RWTH Aachen University, [†]German Research Center of Artificial Intelligence (DFKI)

Abstract—As a promising technology, physical layer security (PLS) enhances security by leveraging the physical characteristics of communication channels. However, the conventional PLS approach leads to a considerable disparity in the effort legitimate users need to secure data compared to eavesdroppers. To address this issue, we propose a physical layer deception (PLD) framework, which applies random deceptive ciphering and orthogonal frequency-division multiplexing (OFDM) to defend against eavesdropping proactively. While ensuring the same level of confidentiality as traditional PLS methods, the PLD approach additionally introduces a deception mechanism, even when the eavesdropper possesses the same knowledge about the transmitter end as the legitimate receiver. Through thorough theoretical analyses and numerical simulations, we prove the superiority of our method over the conventional PLS approach.

Index Terms—Physical layer security, cyber deception, OFDM, finite blocklength codes.

I. INTRODUCTION

Physical layer security (PLS) has gained significant attention as a rising area of interest in wireless systems. Unlike traditional cryptographic methods, PLS exploits the characteristics of the physical channel and offers an additional layer of protection against eavesdropping. As an effective complement to traditional methods, PLS is becoming increasingly crucial in contemporary wireless networks [1].

Although most research on PLS focus on infinite blocklength codes, it is crucial and necessary to exploit the PLS on the finite blocklength (FBL) due to the future trend of ultra-reliable low-latency communication (URLLC) [2], where the data packet only consist of a small number of bits to support extremely reliable transmission with minimal latency. To access PLS performance with FBL, the authors in [3] establish the bounds for the achievable security rate considering a specified leakage probability and error probability. Efforts such like [4]–[6] have been made to explore FBL regime for PLS. Furthermore, authors in [7] investigate the maximal secrecy rate over a wiretap channel and its tightest bounds for both discrete memoryless and Gaussian channels. The authors in [8] maximize the secrecy rate under the covertness constraint by maintaining the confidential signal’s signal-to-noise ratio below a certain threshold in the wiretap channel, preventing eavesdroppers from detecting the transmission. The interplay between reliability and security is studied in [9], where the joint secure-reliability performance is improved by optimizing the allocation of transmission resources. In [10], the idea of exchanging reliability for security is introduced to describe the trade-off between security and reliability in PLS for short-packet transmissions.

However, the passive nature of PLS results in a notable imbalance between the legitimate users and the eavesdroppers, as the eavesdroppers can always try to wiretap with little risk of being detected while the legitimate users should take more precautions to secure data. To make up for this shortcoming, active defense methods should be introduced to PLS, such as deception technologies, which aim to confuse and distract potential eavesdroppers by creating false data or environments, thereby securing the real information. The principles of deception were initially introduced by *Mitnick* [11] in the field of social engineering and then adapted into defensive strategies, which were called *honeypots* and then expanded to a wider range of deception technologies [12]. However, in the physical layer of wireless systems, deception technologies are still in the early stages of development. In [13], the spatial diversity of multi-input multi-output (MIMO) is utilized to lure an eavesdropper into a trap area where the fake messages are received. The authors in [14] design a generative adversarial network (GAN) to generate waveforms that disrupt the eavesdropper’s recognition model.

We proposed a novel framework of physical layer deception (PLD) [15] in 2023, where non-orthogonal multi-access (NOMA) was applied to enhance security. This framework was the first to integrate NOMA-based PLS with deception technologies. We optimized the encryption rate and the power allocation jointly to achieve high secure reliability and effective deception. We further improve the optimization problem in [16], where we maximized the effective deception rate under the constraint of leakage-failure probability (LFP) instead of directly combining the secrecy performance and deception performance. We also detailed the system model with both activated and deactivated ciphering and provided a comprehensive reception error model in different scenarios.

In this work, we extend our previous work and investigate the performance of orthogonal frequency-division multiplexing (OFDM)-based PLD framework. Instead of optimizing the deception rate by setting the constraint of LFP, we consider the constraint of throughput so that a high deception rate can be attained while ensuring the security and efficiency of the transmission. By jointly optimizing the channel coding rates of ciphertext and key, we achieve a high deception rate while maintaining LFP as low as in the conventional PLS method.

The remaining part of this paper is structured as follows. We begin with setting up the system model and optimization problem in Sec. II. Afterward, we present our theoretical analyses and our optimization algorithm in Sec. III. In Sec. IV, our approach is numerically validated and evaluated. Finally, we conclude our paper and provide outlooks in Sec. V.

II. PROBLEM SETUP

A. System Model

We consider an end-to-end communication system where the information source *Alice* sends messages to the receiver *Bob* over wireless channel h_{Bob} with gain $z_{\text{Bob}} = |h_{\text{Bob}}|^2$. At the same time, an eavesdropper *Eve* listens to *Alice* over the eavesdropping channel h_{Eve} with gain $z_{\text{Eve}} = |h_{\text{Eve}}|^2$. With proper beamforming, *Alice* can keep h_{Bob} statistically superior to h_{Eve} , which is a necessary condition of PLS feasibility. Our framework is illustrated in Fig. 1, where *Alice* applies a two-stage encoder followed by OFDM-based waveforming.

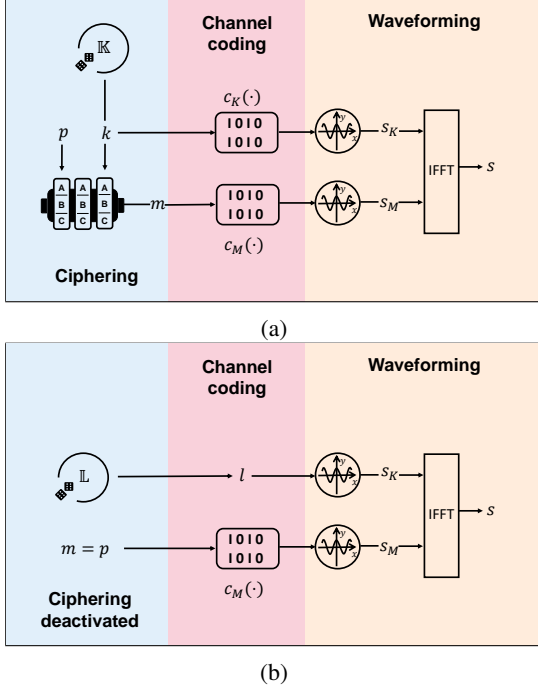


Fig. 1: The transmitting scheme of *Alice*, with deceptive ciphering (a) activated and (b) deactivated, respectively.

In this framework, the cipherer can be activated and deactivated by option. When activated, the d_P -bit plaintext p with is encrypted into a d_M -bit ciphertext using a d_K -bit key k :

$$m = f(p, k) \in \mathbb{M}, \quad \forall (p, k) \in (\mathbb{P} \times \mathbb{K}), \quad (1)$$

where $\mathbb{M} \subseteq \{0, 1\}^{d_M}$, $\mathbb{P} \subseteq \{0, 1\}^{d_P}$, and $\mathbb{K} \subseteq \{0, 1\}^{d_K}$ are the feasible sets of ciphertext codes, plaintext codes, and keys, respectively. On the other hand, given the chosen key k , the plaintext can be decrypted from the ciphertext through $p = f^{-1}(m, k)$. Especially, the codebooks shall be designed to ensure $\mathbb{M} \subseteq \mathbb{P}$, and that $\forall (m, k, k') \in (\mathbb{M} \times \mathbb{K}^2)$ it holds $f^{-1}(m, k') \big|_{k' \neq k} \neq f^{-1}(m, k)$.

The second stage is channel coding, where error correction redundancies are attached to both m and k , respectively. The two output codewords are then individually modulated using OFDM. On the receiver side, for both $i \in \{\text{Bob}, \text{Eve}\}$, it holds $r_i = s_i * h_i + w_i$, where s is the power-normalized baseband signal to transmit, r_i and w_i are the baseband signal and equivalent baseband noise received at i , respectively.

On the other hand, when the cipherer is deactivated, the plaintext p is directly inherited as the ciphertext, i.e., $m = p$. Meanwhile, instead of a valid ciphering key $k \in \mathbb{K}$, a ‘‘litter’’ sequence $l \in \mathbb{L}$ is generated randomly to derive s_K . Particularly, the set of litter codes $\mathbb{L} \subseteq \{0, 1\}^n$ shall fulfill

$$\exists \{k, l\} \in \mathbb{K} \times \mathbb{L} : D_{\text{Hammm}}(c_K(k), l) \leq D_{\text{max}}, \quad (2)$$

where $D_{\text{Hammm}}(x, y)$ is the Hamming distance between x and y , and D_{max} is the maximal distance of a received codeword from the codebook for the channel decoder c_K^{-1} to correct errors. The waveforming stage remains the same like with the deceptive cipherer activated.

Challenging the worst case where *Eve* has maximum knowledge of this framework, we assume that the tuple $(\mathbb{P}, \mathbb{M}, \mathbb{K}, f, f^{-1})$, as well as the modulation and channel coding schemes, are all *common knowledge* shared among *Alice*, *Bob*, and *Eve*. Assuming that both *Bob* and *Eve* have perfect knowledge of their own channels so that ideal channel equalization is achieved.

B. Error Model

When the deceptive ciphering is activated, there can be three possible outcomes for decoding both the m and k :

- 1) *Success*: When the bit errors fall within the error correction capacity of the channel decoder, the data is retrieved.
- 2) *Erasure*: If the bit errors surpass the receiver’s error correction ability but not its error detection capacity, the receiver will recognize and report an erasure.
- 3) *Error*: If the bit errors exceed the error detection capability, the receiver will incorrectly decode the data, resulting in an undetected packet error.

Practically, if *Alice* is properly configured to encode both m and k with enough redundancy and transmit with sufficient power, undetected error is unlikely to occur. Thus, there are three possible deciphering outcomes, as represented in Tab. I.

- 1) *Perception*: If both m and k are successfully decoded, the plaintext p is correctly perceived.
- 2) *Loss*: With m erased, the receiver cannot decrypt regardless its reception of k , resulting in the loss of the p .
- 3) *Deception*: If the ciphering mechanism is randomly activated on selected messages (e.g., the most confidential ones), the deception can occur when the receiver successfully decodes m but have k erased. In this scenario, the receiver, unaware of whether the cipherer is active, cannot determine if the issue is caused by a transmission error or if the cipherer is inactive (meaning no k but a random l was transmitted). If the receiver mistakenly assumes the former as the latter, it will interpret the ciphertext as unciphered plaintext, leading to deception.

C. Performance Metrics

Conventional PLS approaches, which primarily operate in the infinite blocklength (IBL) regime, often rely on secrecy capacity to assess security performance. However, in the FBL regime, the conventional notion of channel

		Ciphertext	
		Success	Erasure
Key	Success	Perception	Loss
	Erasure	Deception	Loss

TABLE I: Reception error model of the proposed approach with random cipherer activation.

capacity is no longer applicable, as error-free transmission is rarely attainable [3]. As an alternative performance indicator for secure and reliable communication, we introduce the LFP $\varepsilon_{\text{LF}} = 1 - (1 - \varepsilon_{\text{Bob}})\varepsilon_{\text{Eve}}$, i.e. the probability that the plaintext is either correctly perceived by *Eve*, or not perceived by *Bob*. Here, ε_{Bob} and ε_{Eve} are the non-perception probabilities of *Bob* and *Eve*, respectively. Notating as $\varepsilon_{i,j}$ the erasure probability of receiver $i \in \{\text{Bob}, \text{Eve}\}$ at decoding the message component $j \in \{\text{M}, \text{K}\}$, we have $\varepsilon_i = 1 - (1 - \varepsilon_{i,\text{M}})(1 - \varepsilon_{i,\text{K}})$ and therefore $\varepsilon_{\text{LF}} = 1 - (1 - \varepsilon_{\text{Bob},\text{M}})(1 - \varepsilon_{\text{Bob},\text{K}})[1 - (1 - \varepsilon_{\text{Eve},\text{M}})(1 - \varepsilon_{\text{Eve},\text{K}})]$. Additionally, to evaluate the performance of deceiving eavesdroppers, we define the effective deception rate as the probability that not *Bob* but only *Eve* is deceived, i.e., $R_d = [1 - (1 - \varepsilon_{\text{Bob},\text{M}})\varepsilon_{\text{Bob},\text{K}}](1 - \varepsilon_{\text{Eve},\text{M}})\varepsilon_{\text{Eve},\text{K}}$. According to [17], the error probability $\varepsilon_{i,j}$ with a given packet size d_j can be written as $\varepsilon_{i,j} = Q\left(\sqrt{\frac{n_j}{V(\gamma_i)}}(\mathcal{C}(\gamma_i) - \frac{d_j}{n_j})\ln 2\right)$, where $Q(x) = \frac{1}{\sqrt{2\pi}}\int_x^\infty e^{-t^2/2}dt$ is the Q-function in statistic, $\mathcal{C}(\gamma_i) = \log_2(1 + \gamma_i)$ is the Shannon capacity, $V(\gamma_i) = 1 - \frac{1}{(1+\gamma_i)^2}$ is the channel dispersion with $\lambda_i = \frac{z_i P}{\sigma^2}$.

D. Strategy Optimization

For convenience of analysis, we assume the subcarriers are allocated to the ciphertext and the key equally. The duration of the cyclic prefix is set to 0 and the bandwidth is normalized to 1. The modulation scheme of ciphertext and key is BPSK. Thus, the throughput is $T = (1 - \varepsilon_{\text{LF}})\left(\frac{d_{\text{M}}}{n_{\text{M}} + n_{\text{K}}}\right)$. In order to pursue secure and efficient transmission, we maximize the effective deception rate while maintaining high throughput. The ciphertext length d_{M} and the key length d_{K} are fixed to simplify the encryptor design, while their coding rates are adjustable to ensure efficient transmission. Thus, the optimization problem can be represented as:

$$(OP) : \underset{n_{\text{M}}, n_{\text{K}}}{\text{maximize}} \quad R_d \quad (3a)$$

$$\text{subject to} \quad n_{\text{M}}, n_{\text{K}} \in \mathbb{Z}^+, \quad (3b)$$

$$\varepsilon_{\text{Bob},\text{M}} \leq \varepsilon_{\text{Bob},\text{M}}^{\text{th}}, \quad (3c)$$

$$\varepsilon_{\text{Eve},\text{M}} \leq \varepsilon_{\text{Eve},\text{M}}^{\text{th}}, \quad (3d)$$

$$\varepsilon_{\text{Bob},\text{K}} \leq \varepsilon_{\text{Bob},\text{K}}^{\text{th}}, \quad (3e)$$

$$\varepsilon_{\text{Eve},\text{K}} \geq \varepsilon_{\text{Eve},\text{K}}^{\text{th}}, \quad (3f)$$

$$T \geq T^{\text{th}} \quad (3g)$$

III. PROPOSED APPROACH

A. Analyses

The original problem (3) is challenging to solve due to the non-convexity of R_d . Therefore, we reformulate it into

a simpler but equivalent version. Based on our analytical insights, we demonstrate that the objective function exhibits partial convexity with respect to each optimization variable.

We first relax n_{M} and n_{K} from integers to real values:

$$\underset{n_{\text{M}}, n_{\text{K}}}{\text{maximize}} \quad R_d \quad (4a)$$

$$\text{subject to} \quad n_{\text{M}}, n_{\text{K}} \in \mathbb{R}^+, \quad (4b)$$

$$(3c) - (3g) \quad (4c)$$

Subsequently, the original problem can be decomposed with:

Lemma 1. For a given $(\hat{n}_{\text{M}}^{(q)}, \hat{n}_{\text{N}}^{(q)})$, R_d is lower-bounded by an approximation $\hat{R}_d(n_{\text{M}}, n_{\text{K}} | \hat{n}_{\text{M}}^{(q)}, \hat{n}_{\text{N}}^{(q)})$, i.e.,

$$\begin{aligned} R_d(n_{\text{M}}, n_{\text{K}}) &= [1 - (1 - \varepsilon_{\text{Bob},\text{M}})\varepsilon_{\text{Bob},\text{K}}](1 - \varepsilon_{\text{Eve},\text{M}})\varepsilon_{\text{Eve},\text{K}} \\ &\geq \left[1 - \left(1 - \hat{\varepsilon}_{\text{Bob},\text{M}}(\hat{n}_{\text{M}}^{(q)}, \hat{n}_{\text{K}}^{(q)})\right)\varepsilon_{\text{Bob},\text{K}}\right] \\ &\quad \cdot \left((1 - \varepsilon_{\text{Eve},\text{M}})\hat{\varepsilon}_{\text{Eve},\text{K}}(\hat{n}_{\text{M}}^{(q)}, \hat{n}_{\text{K}}^{(q)})\right) \\ &\triangleq \hat{R}_d(n_{\text{M}}, n_{\text{K}} | \hat{n}_{\text{M}}^{(q)}, \hat{n}_{\text{K}}^{(q)}) \end{aligned} \quad (5)$$

where $\hat{\varepsilon}_{\text{Bob},\text{M}}(\hat{n}_{\text{M}}^{(q)}, \hat{n}_{\text{K}}^{(q)}) = 1 - b(-\hat{\omega})e^{-a(-\hat{\omega})\omega_{\text{M}}} - c(-\hat{\omega})$ and $\hat{\varepsilon}_{\text{Eve},\text{K}}(\hat{n}_{\text{M}}^{(q)}, \hat{n}_{\text{K}}^{(q)}) = 1 - b(-\hat{\omega})e^{-a(-\hat{\omega})\omega_{\text{K}}} - c(-\hat{\omega})$.

Proof. Eq. (5) can be obtained from the approximation of the Q-function according to lemma 3 in [10]. We introduce and auxiliary function $\omega = \sqrt{\frac{n}{V(\lambda)}}(\mathcal{C}(\lambda) - \frac{d}{n})\ln 2$. For a given $\hat{\omega} \in \mathcal{R}$, Q-function is bounded by $1 - b(-\hat{\omega})e^{-a(-\hat{\omega})\omega} - c(-\hat{\omega}) \leq Q(\omega) \leq b(\hat{\omega})e^{-a(\hat{\omega})\omega} + c(\hat{\omega})$, where $a(\hat{\omega}) = \max\left\{\frac{e^{-\frac{(\hat{\omega})^2}{2}}}{\sqrt{2\pi}Q(\hat{\omega})}, \hat{\omega}\right\} > 0$, $b(\hat{\omega}) = \frac{1}{\sqrt{2\pi}\hat{a}}e^{\hat{a}\hat{\omega} - \frac{(\hat{\omega})^2}{2}} > 0$, and $c(\hat{\omega}) = Q(\hat{\omega}) - \hat{b}e^{-\hat{a}\hat{\omega}}$. The equality is taken for $\omega = \hat{\omega}$. \square

In Eq. (5), R_d reaches the lower-bound \hat{R}_d at the point $(\hat{n}_{\text{M}}^{(q)}, \hat{n}_{\text{K}}^{(q)})$, which inspires us to utilize the Majorize-Minimization (MM) algorithm combining with the block coordinate descent (BCD) [18] method to solve the problem. Thus, we first decompose the problem in each t^{th} iteration by fixing n_{M} . The corresponding problem is given by:

$$\underset{n_{\text{K}}}{\text{maximize}} \quad \hat{R}_d^{(t)}(n_{\text{K}} | \hat{n}_{\text{M}}^{(q)}, \hat{n}_{\text{K}}^{(q)}) \quad (6a)$$

$$\text{subject to} \quad n_{\text{M}} = n_{\text{M}}^{(t)}, \quad (6b)$$

$$n_{\text{M}}, n_{\text{K}} \in \mathbb{R}^+, \quad (6c)$$

$$(3c) - (3g). \quad (6d)$$

Next, we leverage the fractional programming (FP) [19] to further decouple the problem. In this way, Problem (6) is equivalent to the following problem:

$$(SP1) : \underset{n_{\text{K}}, y}{\text{maximize}} \quad \hat{f}^{(t)}(n_{\text{K}}, y | \hat{n}_{\text{M}}^{(q)}, \hat{n}_{\text{K}}^{(q)}) \quad (7a)$$

$$\text{subject to} \quad n_{\text{M}} = n_{\text{M}}^{(t)}, \quad (7b)$$

$$n_{\text{M}}, n_{\text{K}} \in \mathbb{R}^+, \quad (7c)$$

$$(3c) - (3g), \quad (7d)$$

where

$$\begin{aligned} & \hat{f}^{(t)} \left(n_K, y | \hat{n}_M^{(q)}, \hat{n}_K^{(q)} \right) \\ &= 2y \sqrt{ \left[1 - \left(1 - \hat{\varepsilon}_{\text{Bob},M}^{(t)}(\hat{n}_M^{(q)}, \hat{n}_K^{(q)}) \right) \varepsilon_{\text{Bob},K} \right]} \\ & - y^2 \frac{1}{ \left(1 - \varepsilon_{\text{Eve},M}^{(t)} \hat{\varepsilon}_{\text{Eve},K}(\hat{n}_M^{(q)}, \hat{n}_K^{(q)}) \right)}. \end{aligned} \quad (8)$$

Theorem 1. Eq. (8) is concave in n_K for fixed y .

Proof. See Appendix A. \square

In Problem (SP1), we introduce an additional variable y and construct the quadratic transform which is concave for fixed y and n_K separately. Thus, we can solve this problem via the BCD method and find the optimal solution n_K° efficiently.

On the other hand, we have the second decomposed problem in the t^{th} iteration by fixing n_K :

$$\text{maximize}_{n_M} \quad \hat{R}_d^{(t)} \left(n_M | \hat{n}_M^{(q)}, \hat{n}_K^{(q)} \right) \quad (9a)$$

$$\text{subject to} \quad n_K = n_K^{(t)}, \quad (9b)$$

$$n_M, n_K \in \mathbb{R}^+, \quad (9c)$$

$$(3c) - (3g). \quad (9d)$$

Similarly, Problem (9) can be reformulated as:

$$(SP2): \text{maximize}_{n_M, y} \quad \hat{g}^{(t)} \left(n_M, y | \hat{n}_M^{(q)}, \hat{n}_K^{(q)} \right) \quad (10a)$$

$$\text{subject to} \quad n_K = n_K^{(t)}, \quad (10b)$$

$$n_M, n_K \in \mathbb{R}^+, \quad (10c)$$

$$(3c) - (3g), \quad (10d)$$

where

$$\begin{aligned} & \hat{g}^{(t)} \left(n_M, y | \hat{n}_M^{(q)}, \hat{n}_K^{(q)} \right) \\ &= 2y \sqrt{ \left(1 - \varepsilon_{\text{Eve},M} \hat{\varepsilon}_{\text{Eve},K}(\hat{n}_M^{(q)}, \hat{n}_K^{(q)}) \right)} \\ & - y^2 \frac{1}{ \left[1 - \left(1 - \hat{\varepsilon}_{\text{Bob},M}(\hat{n}_M^{(q)}, \hat{n}_K^{(q)}) \right) \varepsilon_{\text{Bob},K} \right]}. \end{aligned} \quad (11)$$

Theorem 2. Eq. (11) is concave in n_M for fixed y .

Proof. See Appendix B. \square

Therefore, we can also solve Problem (10) via BCD approach and obtain the optimal solution n_M° .

B. Optimization Algorithm

Based on the above analyses, we propose an algorithm with three layers of iterations. In the q^{th} iteration, we approximate $\hat{R}_d^{(q)} := \hat{R}_d \left(\hat{n}_M^{(q)}, \hat{n}_K^{(q)} \right)$. Next, we fix the value of n_M and n_K respectively in t^{th} iteration. In this way, we can solve the single-variable problem via FP approach, which is equivalent to solving problem (SP1) and (SP2). In particular, in the inner i^{th} iteration for fixed $n_M^{(t)}$, the optimal $y^{(i)}$ can be found in a closed form for fixed $n_K^{(t-1)}$. And $n_K(i)$ can be updated

by solving the reformulated convex optimization problem. Furthermore, we can use the same way to calculate the optimal $n_M^{(t)}$. Then the local point $(n_M^{(t)}, n_K^{(t)})$ will be assigned to $(n_M^{(q+1)}, n_K^{(q+1)})$ for the next $(q+1)^{\text{th}}$ iteration. The process is repeated until the relative error is less than the threshold or the maximum number of iterations is achieved.

Algorithm 1: The proposed MM-FP framework

```

1 Input:  $\mu_{\text{BCD}}, \mu_{\text{MM}}, \mu_{\text{FP}}, T, Q, I, J, P, n_M, n_K$ 
2 Initialize:  $t = 1, q = 1, i = 1, j = 1, n_M^{(0)} = n_M^{\text{init}}, n_K^{(0)} = n_K^{\text{init}}, \hat{n}_M^{(0)} = \hat{n}_M^{\text{init}}, \hat{n}_K^{(0)} = \hat{n}_K^{\text{init}}, R_d^{(0)} = -\infty$ 
3 do
4   if  $q \leq Q$  then
5      $t \leftarrow 1$  (reset index  $t$ )
6      $\hat{f}^{(t)} := \hat{f} \left( \hat{n}_M^{(q)}, \hat{n}_K^{(q)} \right), \hat{g}^{(t)} := \hat{g} \left( \hat{n}_M^{(q)}, \hat{n}_K^{(q)} \right)$ 
7     do
8       if  $t \leq T$  then
9         do
10           $i \leftarrow 1$  (reset index  $i$ )
11          if  $i \leq I$  then
12             $y^{(i)} = \frac{\sqrt{\left[ 1 - \left( 1 - \varepsilon_{\text{Bob},M}^{(t-1)} \right) \varepsilon_{\text{Bob},K} \left( n_K^{(i-1)} \right) \right]}}{\left( 1 - \varepsilon_{\text{Eve},M}^{(t-1)} \right) \hat{\varepsilon}_{\text{Eve},K} \left( n_K^{(i-1)} \right)}$ 
13             $n_K^{(i)} \leftarrow \arg \max_{n_K} \hat{f} \left( y^{(i)}, n_M^{(t-1)} \right)$ 
14             $i \leftarrow i + 1$ 
15          else
16            break
17          end
18          while  $\frac{\hat{f}^{(i)} - \hat{f}^{(i-1)}}{\hat{f}^{(i-1)}} > \mu_{\text{FP}}$ ;
19           $n_K^{(t)} \leftarrow n_K^{(i)}$ 
20          do
21             $j \leftarrow 1$  (reset index  $j$ )
22            if  $j \leq J$  then
23               $y^{(j)} = \frac{\sqrt{\left( 1 - \varepsilon_{\text{Eve},M}^{(j-1)} \right) \hat{\varepsilon}_{\text{Eve},K} \left( n_K^{(t)} \right)}}{\left[ 1 - \left( 1 - \varepsilon_{\text{Bob},M}^{(j-1)} \right) \varepsilon_{\text{Bob},K} \left( n_K^{(t)} \right) \right]}$ 
24               $n_M^{(j)} \leftarrow \arg \max_{n_M} \hat{g} \left( y^{(j)}, n_K^{(t)} \right)$ 
25               $j \leftarrow j + 1$ 
26            else
27              break
28            end
29            while  $\frac{\hat{g}^{(j)} - \hat{g}^{(j-1)}}{\hat{g}^{(j-1)}} > \mu_{\text{FP}}$ ;
30             $n_M^{(t)} \leftarrow n_M^{(j)}$ 
31             $\hat{R}_d^{(t)} \leftarrow \hat{R}_d \left( n_M^{(t)}, n_K^{(t)} \right), t \leftarrow t + 1$ 
32          else
33            break
34          end
35          while  $\frac{\hat{R}_d^{(t)} - \hat{R}_d^{(t-1)}}{\hat{R}_d^{(t-1)}} > \mu_{\text{BCD}}$ ;
36           $\hat{n}_M^{(q)} \leftarrow n_M^{(t)}, \hat{n}_K^{(q)} \leftarrow n_K^{(t)}, q \leftarrow q + 1$ 
37        else
38          break
39        end
40      while  $\frac{\hat{R}_d^{(t)} \left( \hat{n}_M^{(q)}, \hat{n}_K^{(q)} \right) - \hat{R}_d^{(t)} \left( \hat{n}_M^{(q-1)}, \hat{n}_K^{(q-1)} \right)}{\hat{R}_d^{(t)} \left( \hat{n}_M^{(q-1)}, \hat{n}_K^{(q-1)} \right)} > \mu_{\text{MM}}$ ;
41       $n_M^* \leftarrow \arg \max_{n \in \{ \lfloor n_M^{(q)} \rfloor, \lceil n_M^{(q)} \rceil \}} R_d \left( n, n_K^{(q)} \right)$ 
42       $n_K^* \leftarrow \arg \max_{n \in \{ \lfloor n_K^{(q)} \rfloor, \lceil n_K^{(q)} \rceil \}} R_d \left( n_M^*, n \right)$ 
43      return  $(n_M^*, n_K^*)$ 

```

Specifically, the initial values of n_M and n_K should be feasible for Problem (OP). Besides, since both n_M and n_K must be integers, the optimal solution must be determined by comparing the integer neighbors of n_M^* and n_K^* .

IV. NUMERICAL EVALUATION

To verify our analyses and assess the proposed approach, a series of numerical experiments were performed. The general parameters of the simulation setup are presented in Tab. II, while task-specific parameters will be explained later.

TABLE II: Simulation setup

Parameter	Value	Remark
σ^2	1 mW	Noise power
B	1 Hz	Normalized to unity bandwidth
d_M	16 bits	Length of ciphertext
d_K	16 bits	Length of key
$\varepsilon_{\text{Bob},M}^{\text{th}}$	0.5	Thresholds in constraints (3c)–(3f)
$\varepsilon_{\text{Bob},K}^{\text{th}}$		
$\varepsilon_{\text{Eve},M}^{\text{th}}$		
$\varepsilon_{\text{Eve},K}^{\text{th}}$		
ξ	2×10^{-16}	BCD convergence threshold
K	100	Maximal number of iterations in BCD

A. Deception Rate Surface

We set the transmission power $P = 5$ mW for both ciphertext and key, under the condition that $z_{\text{Bob}} = 0$ dB and $z_{\text{Eve}} = -10$ dB. We calculated R_d in the region $(n_M, n_K) \in [16, 128] \times [16, 128]$ with $T^{\text{th}} = 0.1$ bps. The result in Fig. 2 illustrates the concavity of the deception rate surface in the feasible region, which is constrained by (3b-3f) and highlighted with greater opacity compared to the rest. However, the behavior related to convexity or concavity beyond this region seems to be more complex.

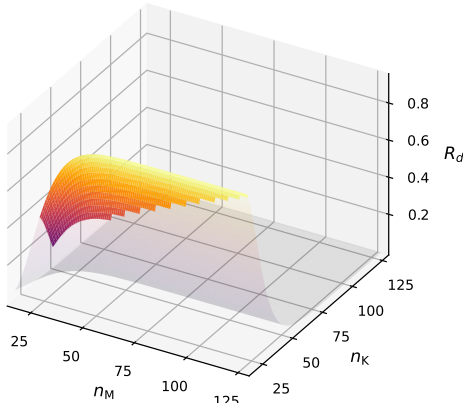


Fig. 2: Deception rate with $T_{\text{LF}}^{\text{th}} = 0.1$ bps.

B. Convergence Test of the Optimization Algorithm

To verify the effectiveness of the proposed BCD algorithm, we conducted Monte-Carlo simulations, where we set $T^{\text{th}} = 0.1$ bps with transmission power $P = 5$ mW, $z_{\text{Bob}} = -5$ dB, $z_{\text{Eve}} = -15$ dB. Fig. 3 illustrates the search path with $d_M = 16$ bits and $d_M = 24$ bits and proves that the BCD algorithm converges at the optimum.

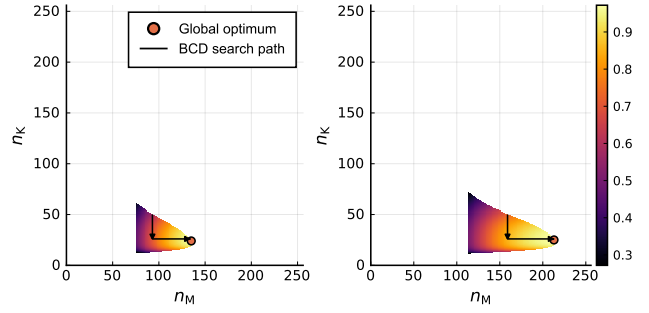


Fig. 3: The R_d surface and the search path with $d_M = 16$ bits (left) and $d_M = 24$ bits (right).

C. Performance Evaluation

To evaluate the secrecy and deception performance of our proposed deception scheme, we calculated ε_{LF} and R_d under varying eavesdropping channel gain z_{Eve} . In this experiment, we set $P = 5$ mW, $z_{\text{Bob}} = 0$ dB, and $T^{\text{th}} = 0.05$. Besides, we also measured the performance of the conventional PLS method as a baseline, which minimizes ε_{LF} with respect to n_M without deceptive ciphering ($d_K = 0$). The results are represented in Fig. 4, which demonstrate that better eavesdropping condition enhances the deception performance. Although the ε_{LF} of our method increases with the growth of z_{Eve} , it still remains at a very low value and performs closely to the baseline.

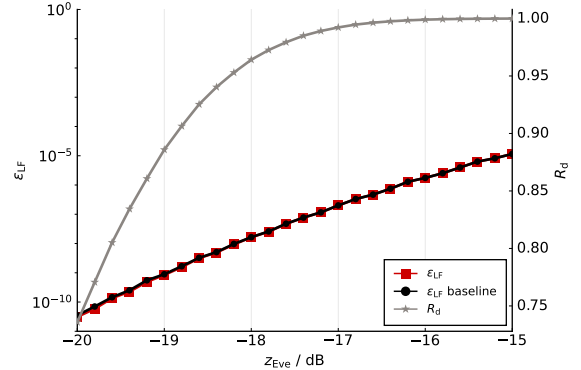


Fig. 4: The impact of z_{Eve} .

Next, we set $z_{\text{Eve}} = -15$ dB, $z_{\text{Bob}} = 0$ dB, $T_{\text{th}} = 0.05$ bps to test the performance w.r.t. the transmission power. The results are shown in Fig. 5, which indicates that the deception performance benefits from higher transmission power, while the ε_{LF} rises logarithmically slowly as the transmission power increases.

Fig. 6 shows the sensitivity of ε_{LF} to the raw packet rate, which is tested under $z_{\text{Bob}} = 0$ dB, $z_{\text{Eve}} = -10$ dB, and $T^{\text{th}} = 0.05$ bps. Compared with the conventional PLS method, our PLD method benefits from a lower raw data rate. As the raw packet rate increases, the deception performance degrades, while the leakage failure probability rises.

The outcome of a comprehensive benchmark test is depicted in Fig. 7, where we combined z_{Eve} and transmission power. We

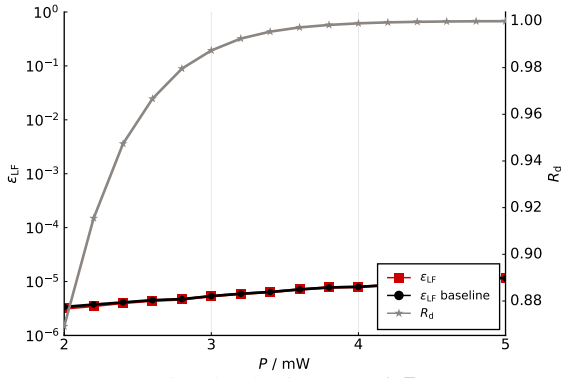


Fig. 5: The impact of P .

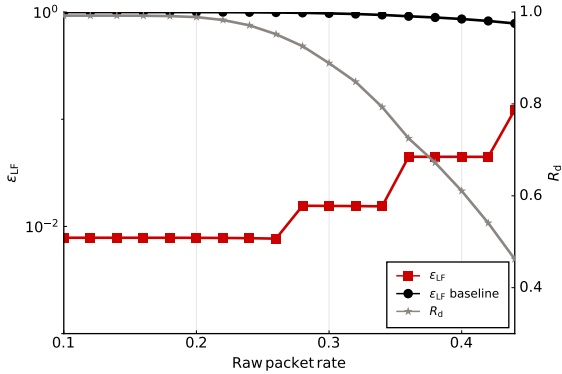


Fig. 6: The impact of raw packet rate.

kept the setup $T^{\text{th}} = 0.05$. The deception rate rises with better eavesdropping channel conditions and higher transmission power. Regarding the ε_{LF} , the PLD method performs closely to the conventional PLS method. The ε_{LF} gets larger as the z_{Eve} and transmission power increase.

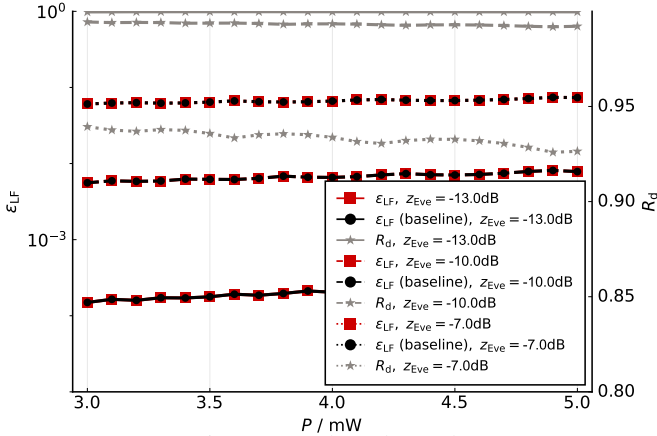


Fig. 7: Benchmark results

V. CONCLUSION AND OUTLOOKS

In this work, we have investigated the performance of our proposed PLD framework with OFDM. By jointly optimizing the coding rate of the ciphertext and the key, we maximized the effective deception rate while maintaining a

specified throughput constraint, thereby ensuring both secure and efficient communication. We have proved the convexity of the objective function and proposed an efficient algorithm to solve the related optimization problem. The comprehensive numerical simulation results have demonstrated that our approach introduced high deception rate without compromising security compared with the conventional PLS method.

REFERENCES

- [1] J. M. Hamamreh *et al.*, "Classifications and applications of physical layer security techniques for confidentiality: A comprehensive survey," *IEEE Commun. Surv. Tutor.*, vol. 21, no. 2, pp. 1773–1828, 2019.
- [2] C. She *et al.*, "A tutorial on ultrareliable and low-latency communications in 6g: Integrating domain knowledge into deep learning," *Proc. IEEE*, vol. 109, no. 3, pp. 204–246, 2021.
- [3] W. Yang *et al.*, "Wiretap channels: Nonasymptotic fundamental limits," *IEEE Trans. Inf. Theory*, vol. 65, no. 7, pp. 4069–4093, 2019.
- [4] B. Liu *et al.*, "Energy-efficient optimization in distributed massive MIMO systems for slicing eMBB and URLLC services," *IEEE Trans. Veh. Technol.*, vol. 72, no. 8, pp. 10 473–10 487, 2023.
- [5] K. Li *et al.*, "Joint uplink and downlink resource allocation toward energy-efficient transmission for URLLC," *IEEE J. Sel. Areas Commun.*, vol. 41, no. 7, pp. 2176–2192, 2023.
- [6] C. Liu *et al.*, "Predictive precoder design for ofds-enabled urllc: A deep learning approach," *IEEE J. Sel. Areas Commun.*, vol. 41, no. 7, pp. 2245–2260, 2023.
- [7] W. Yang *et al.*, "Wiretap channels: Nonasymptotic fundamental limits," *IEEE Trans. Inf. Theory*, vol. 65, no. 7, pp. 4069–4093, 2019.
- [8] C. Wang *et al.*, "Achieving covertness and security in broadcast channels with finite blocklength," *IEEE Trans. Wireless Commun.*, vol. 21, no. 9, pp. 7624–7640, 2022.
- [9] M. Oh *et al.*, "Joint optimization for secure and reliable communications in finite blocklength regime," *IEEE Trans. Wireless Commun.*, vol. 22, no. 12, pp. 9457–9472, 2023.
- [10] Y. Zhu *et al.*, "Trade reliability for security: Leakage-failure probability minimization for machine-type communications in urllc," *IEEE J. Sel. Areas Commun.*, vol. 41, no. 7, pp. 2123–2137, 2023.
- [11] K. D. Mitnick *et al.*, *The art of deception: Controlling the human element of security*. John Wiley & Sons, 2003.
- [12] D. Fraunholz *et al.*, "Demystifying deception technology: A survey," 2018, [Online]. Available: arXiv:1804.06196.
- [13] Q. He *et al.*, "Proactive anti-eavesdropping with trap deployment in wireless networks," *IEEE Trans. Dependable Secure Comput.*, vol. 20, no. 1, pp. 637–649, 2022.
- [14] P. Qi *et al.*, "Adversarial defense embedded waveform design for reliable communication in the physical layer," *IEEE Internet Things J.*, 2024.
- [15] B. Han *et al.*, "Non-orthogonal multiplexing in the FBL regime enhances physical layer security with deception," in *2023 IEEE 24th Int. Workshop Signal Process. Adv. Wirel. Commun. (SPAWC)*, 2023, pp. 211–215.
- [16] W. Chen *et al.*, "Physical layer deception with non-orthogonal multiplexing," 2024, [Online]. Available: arXiv:2407.00750.
- [17] Y. Polyanskiy *et al.*, "Channel coding rate in the finite blocklength regime," *IEEE Trans. Inf. Theory*, vol. 56, no. 5, pp. 2307–2359, 2010.
- [18] P. Tseng, "Convergence of a block coordinate descent method for nondifferentiable minimization," *J. Optim. Theory Appl.*, vol. 109, pp. 475–494, 2001.
- [19] K. Shen *et al.*, "Fractional programming for communication systems—part i: Power control and beamforming," *IEEE Trans. Signal Process.*, vol. 66, no. 10, pp. 2616–2630, 2018.

APPENDIX A
PROOF OF THEOREM 1

Proof. To prove the convexity of $\hat{f}^{(t)}$, we first investigate the monotonicity of $\varepsilon_{i,j}$ with respect to n_j . In particular, we have

$$\frac{\partial \varepsilon_{i,j}}{\partial n_j} = \frac{\partial \varepsilon_{i,j}}{\partial w_{i,j}} \frac{\partial w_{i,j}}{\partial n_j} \leq 0, \quad (12)$$

where

$$\frac{\partial \varepsilon_{i,j}}{\partial w_{i,j}} = \frac{\partial \left(\int_{w_{i,j}}^{\infty} \frac{1}{\sqrt{2\pi}} e^{-\frac{t^2}{2}} dt \right)}{\partial w_{i,j}} = -\frac{1}{\sqrt{2\pi}} e^{-\frac{w_{i,j}^2}{2}} < 0, \quad (13)$$

$$\frac{\partial w_{i,j}}{\partial n_j} = \frac{1}{2} n_j^{-\frac{1}{2}} V_{i,j}^{-\frac{1}{2}} \mathcal{C}_{i,j} \ln 2 + \frac{1}{2} n_j^{-\frac{3}{2}} V_{i,j}^{-\frac{1}{2}} d_j \ln 2 \geq 0. \quad (14)$$

Thus, $\varepsilon_{i,j}$ is monotonically decreasing in n_j . Then, we further investigate the convexity of $\varepsilon_{i,j}$ with respect to n_j , we have

$$\frac{\partial^2 \varepsilon_{i,j}}{\partial n_j^2} = \frac{\partial^2 \varepsilon_{i,j}}{\partial w_{i,j}^2} \underbrace{\left(\frac{\partial w_{i,j}}{\partial n_j} \right)^2}_{\geq 0} + \frac{\partial \varepsilon_{i,j}}{\partial w_{i,j}} \underbrace{\frac{\partial^2 w_{i,j}}{\partial n_j^2}}_{< 0} \geq 0, \quad (15)$$

where

$$\frac{\partial^2 \varepsilon_{i,j}}{\partial w_{i,j}^2} = \frac{w_{i,j}}{\sqrt{2\pi}} e^{-\frac{w_{i,j}^2}{2}} \geq 0, \quad (16)$$

$$\frac{\partial^2 w_{i,j}}{\partial n_j^2} = -\frac{1}{4} n_j^{-\frac{3}{2}} V_{i,j}^{-\frac{1}{2}} \mathcal{C}_{i,j} \ln 2 - \frac{3}{4} n_j^{-\frac{5}{2}} V_{i,j}^{-\frac{1}{2}} d_j \ln 2 \leq 0. \quad (17)$$

Therefore, $\varepsilon_{i,j}$ is convex in n_j . We can further prove the concavity of the first term in $\hat{f}^{(t)}$, where $\left[1 - \left(1 - \hat{\varepsilon}_{\text{Bob},M}^{(t)}(\hat{n}_M^{(q)}, \hat{n}_K^{(q)}) \right) \varepsilon_{\text{Bob},K} \right]$ is concave. Since the square-root function is concave and increasing,

$2y \sqrt{\left[1 - \left(1 - \hat{\varepsilon}_{\text{Bob},M}^{(t)}(\hat{n}_M^{(q)}, \hat{n}_K^{(q)}) \right) \varepsilon_{\text{Bob},K} \right]}$ is concave.

Next, we prove the concavity of $\hat{\varepsilon}_{i,j}$. The first derivative of $\hat{\varepsilon}_{i,j}$ is:

$$\frac{\partial \hat{\varepsilon}_{i,j}}{\partial n_j} = \frac{\partial \hat{\varepsilon}_{i,j}}{\partial w_{i,j}} \underbrace{\frac{\partial w_{i,j}}{\partial n_j}}_{\geq 0} \geq 0, \quad (18)$$

where

$$\frac{\partial \hat{\varepsilon}_{i,j}}{\partial w_{i,j}} = a(-\hat{w})b(-\hat{w})e^{-a(-\hat{w})w_{i,j}} > 0. \quad (19)$$

Then, we further investigate the concavity of $\hat{\varepsilon}_{i,j}$ with respect to n_j , we have

$$\frac{\partial^2 \hat{\varepsilon}_{i,j}}{\partial n_j^2} = \frac{\partial^2 \hat{\varepsilon}_{i,j}}{\partial w_{i,j}^2} \underbrace{\left(\frac{\partial w_{i,j}}{\partial n_j} \right)^2}_{\geq 0} + \frac{\partial \hat{\varepsilon}_{i,j}}{\partial w_{i,j}} \underbrace{\frac{\partial^2 w_{i,j}}{\partial n_j^2}}_{< 0} \leq 0, \quad (20)$$

where

$$\frac{\partial^2 \hat{\varepsilon}_{i,j}}{\partial w_{i,j}^2} = -a^2(-\hat{w})b(-\hat{w})e^{-a(-\hat{w})w} < 0. \quad (21)$$

Therefore, the second term of $\hat{f}^{(t)}$ is concave with respect to n_K . Hence, $\hat{f}^{(t)}$ is concave. It is also trivial to show that all the constraints are either convex or linear, i.e., the feasible set

of Problem (7) is convex. Since the objective function to be maximized is concave and its feasible set is convex, Problem (7) is a convex problem. \square

APPENDIX B
PROOF OF THEOREM 2

Proof. According to the proof in Appendix A, $\varepsilon_{\text{Eve},M}$ is convex and $\hat{\varepsilon}_{\text{Bob},M}^{(t)}$ is concave with respect to n_M . Thus, $\hat{g}^{(t)}$ is concave in n_M . \square